Analysis of Quasi-Elastic e-n and e-p Scattering on Deuterium [DRAFT 2]

Alexander Balsamo

March 27, 2018

Contents

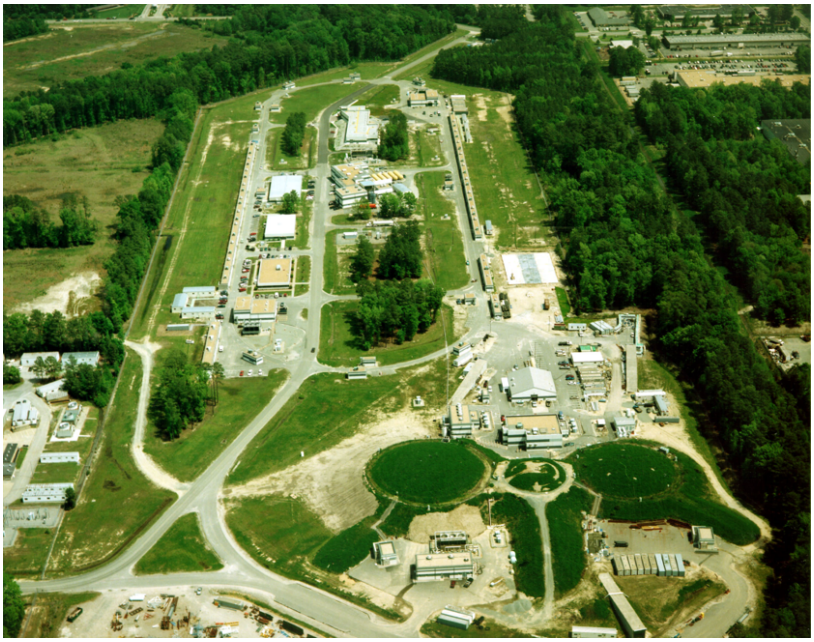

Figure 1: Aerial photo of JLab.

1 Abstract

One of Jefferson Lab's goals is to unravel the quark-gluon structure of nuclei. We will use the ratio, R, of electron-neutron to electron-proton scattering on deuterium to probe the magnetic form factor of the neutron, G_m^n. The G_m^n is a magnetic distribution of charge within the neutron. We have developed an end-to-end analysis from simulation to extraction of R in quasi-elastic kinematics for an approved experiment with the CLAS12 detector. We focus on neutrons detected in the CLAS12 calorimeters and protons measured with the CLAS12 forward detector. Events were generated with the Quasi-Elastic Event Generator (QUEEG) and passed through the Monte Carlo code *gemc* to simulate the CLAS12 response. These simulated events were reconstructed using the latest CLAS12 Common Tools. We first match the solid angle for *e-n* and *e-p* events. The electron information is used to predict the path of QE neutrons and protons through CLAS12. If both particles interact in CLAS12 the *e-n* and *e-p* events have the same solid angle. We select QE events by searching for nuclei near the predicted position based on the scattered electron information. An angular cut between the predicted 3-momentum of the nucleon and the measured value, θ_{pq}, separates QE and inelastic events. We will show the simulated R as a function of the four-momentum transfer Q^2 and use this value to extract the G_m^n.

2 Introduction

2.1 Jefferson Lab

Jefferson Lab (JLab) is a national laboratory located in Newport News, Virginia (Figure 1). JLab is built around the Continuous Electron Beam Accelerator Facility (CEBAF) which is a 12 GeV continuous electron beam that can be routed to one of four analysis halls.

2.1.1 Goals and Motivations

The main goal of JLab is to unravel the quark-gluon structure of nuclei and understand quantum-chromodynamics (QCD) [1]. The motivation of our research is to extract the magnetic form factor of the neutron, G_m^n, using a deuterium target for quasi-elastic kinematics. Electric and magnetic form factors are fundamental observables which reflect the distribution of charge and magnetization within a particle. Although neutrons are neutral, the individual quarks and gluons are not. A campaign has begun at JLab to find the electric and magnetic form factors for the proton and neutron in hopes of unraveling the quark-gluon substructure of nuclei [2].

This goal is accomplished by accelerating an electron beam around a mile long racetrack. 25 cryomodules at temperatures close to 2^oK accelerate the beam, while magnetic fields curve the electrons around the arcs. In the arcs, the beam is moved from highest to lowest arc increasing magnetic field strength as the energy of the beam bucket increases (Figure 2). This beam can than be directed into any of the four detection halls: A, B, C, or D.

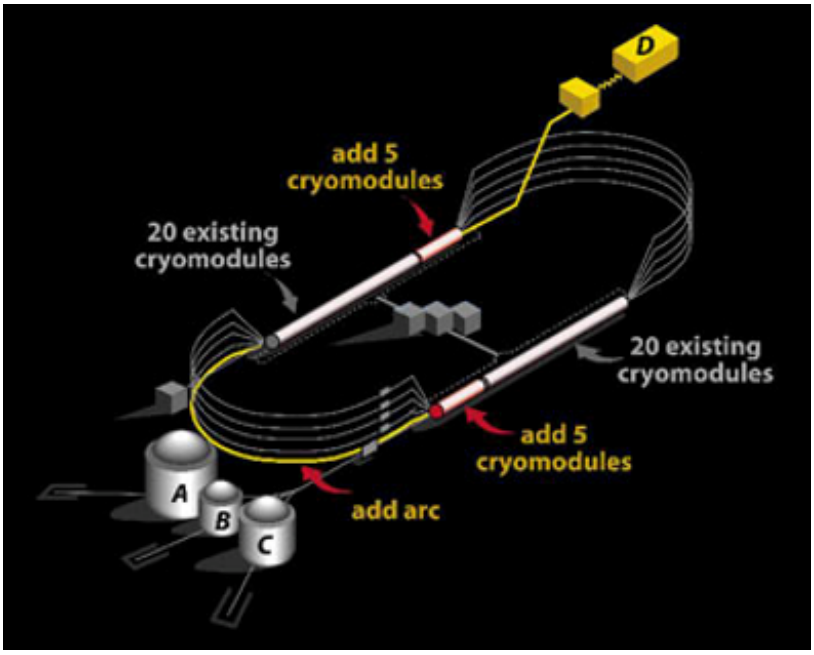

Figure 2: Model of JLab and Halls

JLab has completed an upgrade that doubled the beam energy from 6 GeV to 12 GeV, added Hall D, and built a new detector modeling the previous one in Hall B called the CEBAF Large Acceptance Spectrometer (CLAS12).

3 Detectors and Nuclei Detection

3.1 Hall B and CLAS12

CLAS12 in Hall B is comprised of two detectors: a Central Detector and a Forward Detector. Both of these detectors have smaller detector elements (Figure 3). Using the central and forward detectors, CLAS12 is able to collect data over a wide solid angle as well as measure the 4-momenta of reaction products. The forward detector will be used to extract G_m^n.

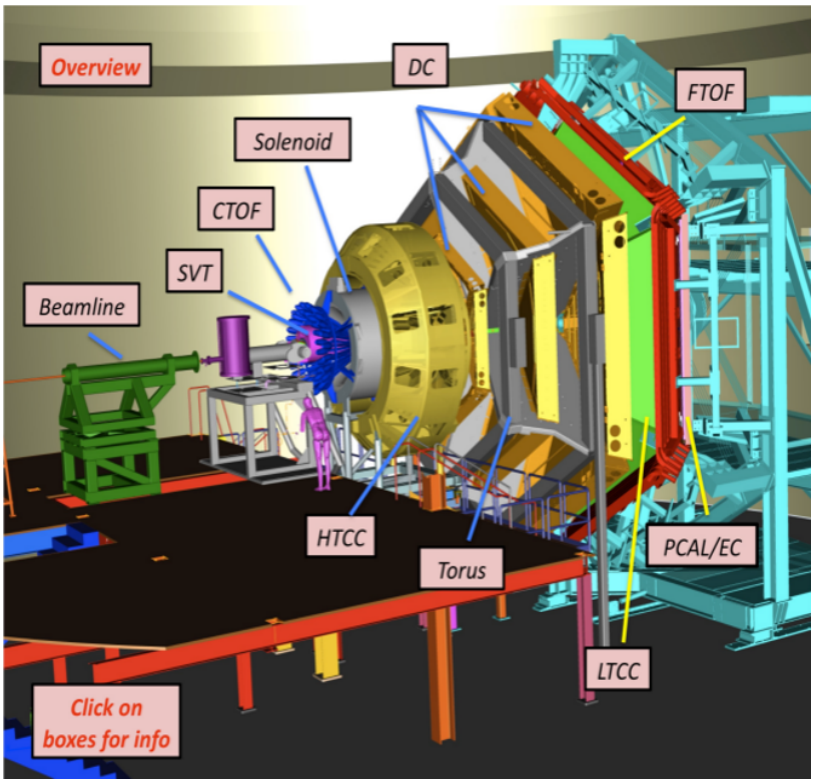

Figure 3: Computer designed image of CLAS12

3.1.1 Torus

The Superconducting Torus is used to generate a toroidal magnetic field in the forward detector. It is a supercooled magnet comprised of six superconducting coils surrounding the beam line, producing a field in the azimuthal direction. By observing which way charged particles bend, we can determine the charge of the particles.

3.1.2 Solenoid

The Superconducting Solenoid is used for data acquisition from large scattering angles in the central detector. The Solenoid is a self-shielded superconducting magnet comprised of 5 coils that produce a field parallel to the beam direction.

3.1.3 Drift Chambers

The Drift Chambers (DC) in the Forward Detectors are used to track charged particle distance and momentum emerging from the target. Each DC is comprised of an array of wires immersed in gas. The placement of the wires forms hexagonal cells as shown in Figure 4. When a charge particle passes through the DC, it ionizes the surrounding gas, producing an electrical signal. The difference between this signal and the start time of the reaction allows us to calculate a radius surrounding each wire (Figure 4). Using the collection of radii we can reconstruct a charged particles path and 4-momenta through the forward detector.

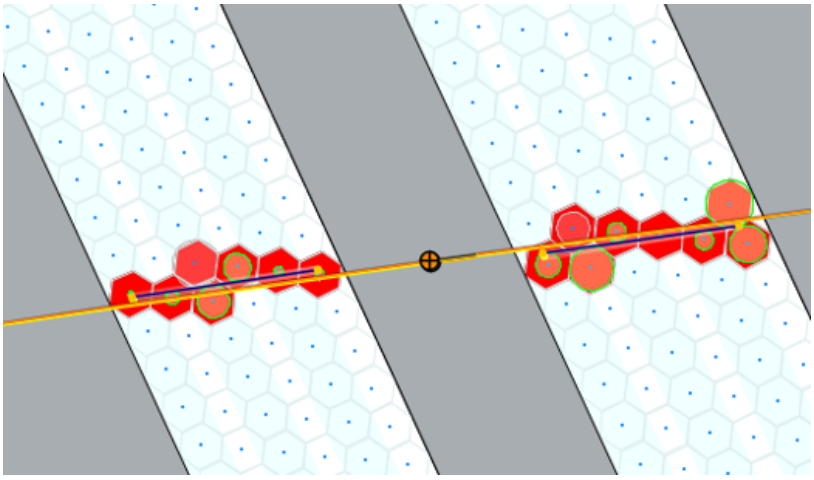

Figure 4: DC detecting ionized gas from charged particle and reconstructing a 3D path

3.1.4 Forward Time-of-Flight

The Forward Time-of-Flight (FTOF) system in the forward detector measures the time-of-flight of charged particles through CLAS12 after the particle passes through the drift chamber. The FTOF is a much more precise measurement of flight time due to scintillators further within the detector having quicker electrical voltage signals. The FTOF includes 6 sectors of plastic scintillators with double sided photomultiplier tubes (PMT). The FTOF in tandem with the DC reconstructs charged particle paths at higher resolutions.

3.1.5 Forward Micromegas

The Forward Micromegas (MICROMEsh GAseous Structure) detector is a gaseous detector on a parallel plate electrode structure used to measure additional track points. The Forward Micromegas are positioned close to the target, allowing for higher resolution of particle path and momentum information.

3.1.6 High and Low Cherenkov Counters

The Low-Threshold and High-Threshold Cherenkov Counters (LTCC and HTCC) are filled with C_4F_{10} gas and an array of PMTs. The HTCC is one unit installed in front of the DC containing mirrors that focus light on eight 5-inch phototubes. The HTCC's main goal is to discern the difference between electrons and π-mesons, specifically those that are negatively charged. This allows for a decrease in background signal and for a more reliable identification of scattered electrons. The LTCC system is used to discern between pions and kaons. When an electron and a π^- pass through the detector, they will both have the same curve from the torus. However, the π^- is of larger mass. When an electron moves through the gas in the Cherenkov Counters, it is of such high momentum and energy that it is moving faster than the speed of light in the gas and produces photons, or Cherenkov radiation, which can be detected. A π^- is heavier and slower, and does not produce Cherenkov radiation as it slows through the Cherenkov Counters. Therefore, if a particle is detected to have negative charge and Cherenkov radiation, we can conclude with a higher certainty that this particle is most likely an electron. If we detect a particle with negative charge that lacks Cherenkov radiation, it is likely a π^-.

3.1.7 Pre-Shower Calorimeter/Electromagnetic Calorimeter

The Pre-Shower Calorimeter/Electromagnetic Calorimeter (PCAL/EC) are used to measure the energies of electrons, protons, and other charged particles. Perhaps most importantly for our analysis, they can also detect the effects of neutrons [4,6]. The PCAL/EC consists of alternating layers of scintillator and lead. The scintillator layer is made of paddles that form triangular shaped sectors (Figure 5a). The strips are rotated 120^o within each set of three layers. Because neutrons are neutral, they do not signal electric currents through the DC or FTOF. In the calorimeters neutrons collide with atomic nuclei and produce a shower of charged particles. This shower produces light in the scintillators that are collected by PMTs. These PMTs in the different layers are used to triangulate the position of the neutron that produced the shower (Figure 5b).

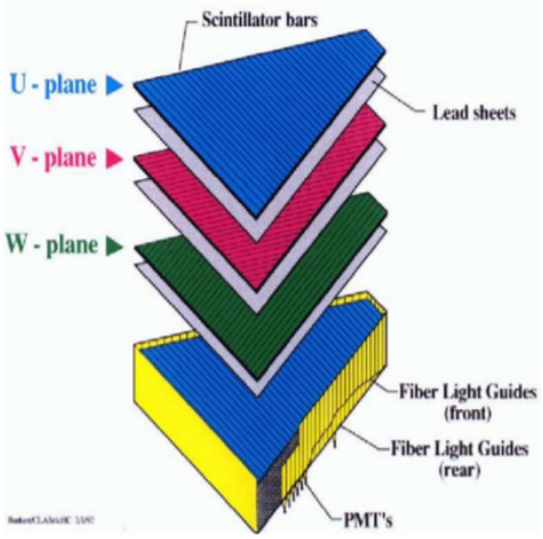

(a) Expanded views of the EC showing lead and scintillator layers

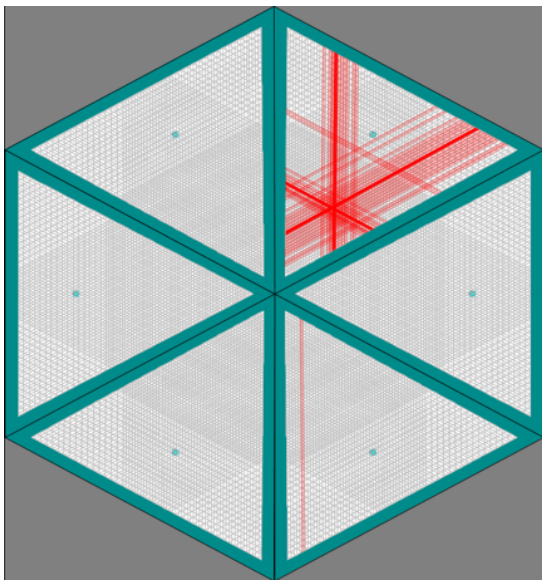

(b) Cross sectional view of PCAL showing triangulation of scintillator bars to locate particle

Figure 5: Neutron Detection in PCAL/EC

3.2 Proton Detection

For our analysis, energy and momentum information was taken primarily from the DC and FTOF to identify protons in electron-proton (e-p) events. Each simulated e-p event was swum through the detector using the toroidal magnetic field to curve the respective particles and the DC and FTOF were used to extract the energy and momentum data. A simulated event in the CLAS Event Display (CED) is shown in Figure 6a. The yellow circles show the position and direction of the track, whereas the curves represent the 3D paths of electrons and protons through CLAS12.

3.3 Neutron Detection

To extract neutron 4-momenta information, the PCAL/EC was used to triangulate a hit point for the neutron. Because neutrons are not effected by the toroidal magnetic field, they move in a straight path through CLAS12. This is clearly shown by the electron-neutron (e-n) event in Figure

6b where a dashed blue line represents the path of a neutron. Also notice how there are no yellow circle hits throughout any point in the DC or FTOF, but there are hits in the PCAL/EC PMTs towards the end of the path.

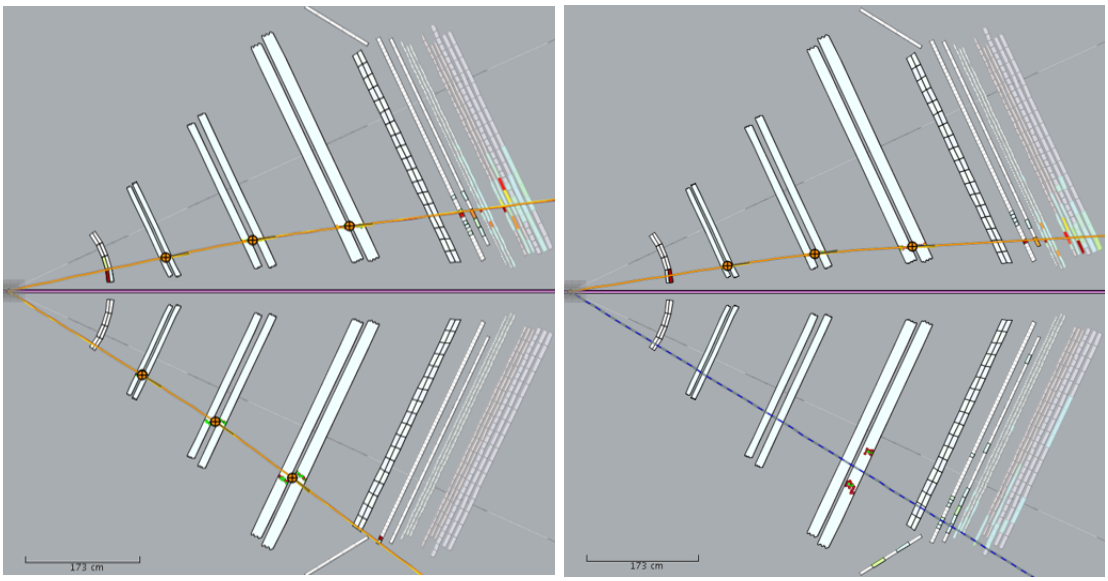

(a) Simulation of found proton (bottom track) through DC/FTOF

(b) Simulation of found neutron (bottom track) hitting PCAL/EC

Figure 6: CED of e-n and e-p events

4 Quasi-Elastic Kinematics

Our analysis of e-n and e-p events focuses on quasi-elastics to extract R and G_m^n. Elasticity is defined as the conservation of 4-momentum in a reaction. The same principle holds true for quasi-elastic kinematics, with a subtle differentiation. For this experiment, we are using a deuterium target. Each atom of deuterium contains a proton and a neutron in its nucleus (Figure 7).

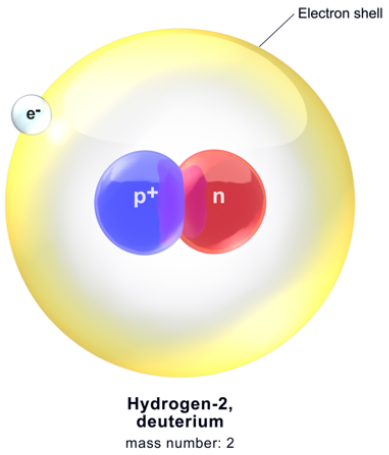

Figure 7: Deuterium atom showing a proton and neutron in the nucleus

The deuterium gives us a neutron target. However, deuterium has two different nucleons in its nucleus which are in contact. The two nucleons experience fermi-motion within the nucleus, and they orbit about each other. This intrinsic rotation changes the center of mass frame between the electron and the nucleon. For example, in an e-p event, if the beam energy was 11 GeV, and the proton was spinning away from the beam, it would appear in the center of mass frame that the beam energy was lower. If the proton was spinning towards the beam, it would appear that we measure a higher elastic energy from proposed theory. Our data in quasi-elastic kinematics should still represent our elastic theory, but the averages will seem to be distributed broadly above and below the average (Figure 8).

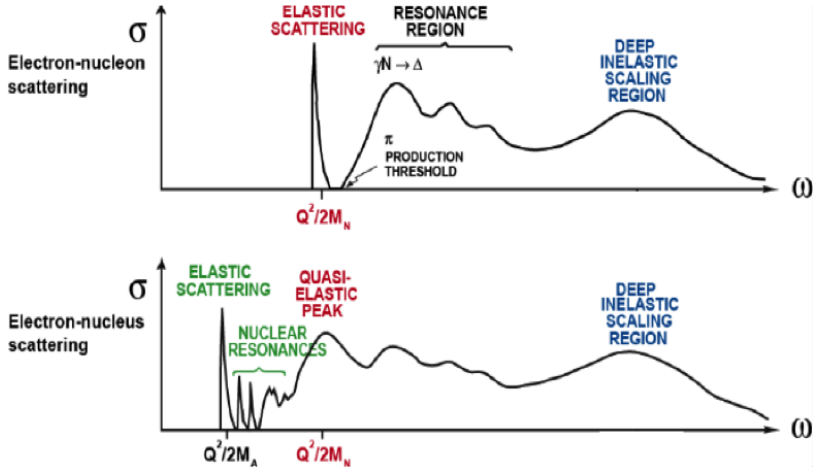

Figure 8: Differentiation between Elastic Scattering (above) and Quasi-Elastic Scattering (below)

5 Method

It is integral to the success of this experiment that once our group is allotted beam time for data collection, that our analysis is ready to extract needed momentum, R, and G_m^n values. We can accomplish this by simulating events using software packages, and then running these simulations through a written analysis using a Java-Scripting Language called *Groovy*. Analyzing a simulation comes with the added benefit of cross checking our extracted values with the known simulated ones. We also can compare data with lower beam energy analysis from earlier experiments with the CLAS6 detector before the upgrade [6]. See Table 1 for a summary of our method.

Program	Purpose
QUEEG	Event Generator
gemc	CLAS12 Simulation
HIPO	Convert to High-Performance data format
Reconstruction	Extract 4-momentum for each track
Analysis	Extract R

Table 1: Summary of methods

The following method is an end-to-end simulation, from generation to extraction, of quasi-elastic e-n and e-p events.

5.1 QUEEG

The QUasi-Elastic Event Generator (QUEEG) is a program written in C++ [3]. QUEEG generates quasi-elastic e-n and e-p 4-momentum vectors based on input beam energy, torus current, minimum and maximum electron scattering angle, and ratio of e-n to e-p events. Since the goal is to extract a ratio of e-n to e-p events, we set the generated ratio to be 0.5 within a minimum angle of 8.0^o, a maximum angle of 37.0^o, and a beam energy of 11.0 GeV. We chose to output the QUEEG file in LUND format, which can be read into the Monte Carlo code *gemc*.

5.2 gemc

The GEant4 Monte Carlo code *gemc* is a C++ program that simulates CLAS12's response for the generated events. Geometry files are read into *gemc* constructing the detector, including its material makeup specific to each detector element, to simulate realistic physics events. Specific detector elements and geometries can be turned on and off; for our simulation, we are primarily concerned with detection in the forward detectors. The output of *gemc* is an evio file, which is a local JLab data format. We can view the constituents of the file using an eviodump command found in the CLAS12 Common Tools (Figure 9).

```
********************** EVENT # 1  **********************
        +----+-----------------------------------+------------+---------+---------+
        |  id|                               name|     entries|    group|    items|
        +----+-----------------------------------+------------+---------+---------+
        |   0|                      MC::Particle|           2|       20|        7|
        |   1|                         FTOF::adc|          54|      101|        7|
        |   2|                         CTOF::adc|          48|      501|        7|
        |   3|                         FTOF::tdc|          54|      102|        5|
        |   4|                         CTOF::tdc|          48|      502|        5|
        |   5|                         ECAL::adc|          81|      201|        7|
        |   6|                         HTCC::adc|           1|      601|        7|
        |   7|                         ECAL::tdc|          81|      202|        5|
        |   8|                       RUN::config|           1|       10|        9|
        |   9|                           DC::tdc|          56|      302|        5|
        |  10|                          DC::doca|          56|      303|        5|
        +----+-----------------------------------+------------+---------+---------+


Choose (n=next,p=previous, q=quit), Type Bank Name or id :
```

Figure 9: Example output of eviodump command showing different databank information

5.3 Convert to HIPO

Evio files output from *gemc* are large, making multiple events and multiple runs of the simulation exceedingly slow and taxing for our computers. By converting to a HIgh Performance Output (HIPO) file format, we can reduce file sizes and increase run time efficiency for each end-to-end simulation. The HIPO file conversion software was written by JLab and is currently running on version 2.0.

5.4 Reconstruction

The HIPO file will than be passed through CLAS12 Reconstruction Common Tools. This program takes the simulated data and determines location, energy, and momentum information individually for each track in each event. This reconstruction outputs data in an array of databanks which can be viewed using the eviodump command. We can then pull the information from the databanks into an analysis code for further investigation and quasi-elastic event selection.

5.5 Analysis

We have written an analysis code using JLab developed *coatjava* packages to read in reconstructed HIPO files and output momentum, energy, and angle information. The algorithm was written using a Java Scripting language called *groovy* and was named protonNeutronThetaPq7.groovy.

The algorithm begins by looping over every possible event in the reconstructed HIPO file. For each event, we check the Time Based Tracking databank (*TimeBasedTrkg::TBTracks*) to see how many particles are in our event. If we observe two particles, we insure that one particle is positively charged and the other is negative; this event is then kept for further investigation. If we observe one particle, and that particle is an electron, we keep this event for further analysis.

We must then match the solid angle for *e-n* and *e-p* events. The electron information is used to predict the trajectory of both a neutron and proton through CLAS12 (Figure 10). If both particles would interact in the CLAS12 volume, we know the sample has the same solid angle for e-n and e-p events. We then select QE events by searching for a nucleon near the predicted position. For e-p events, we use the electron momentum to predicted the scattered proton momentum track through the torus and DC/FTOF. We then check to see if this prediction is close to the observed value. If this is the case, momentum information is extracted from the electron and proton, and used to calculate scatter angles and other results. If the predicted path does not match the observed path, this event is excluded from the analysis. The found reconstructed events can than be compared to the generated events for consistency and checks.

The electron only events are candidates for *e-n* events. Much like the e-p events, we use the electron momentum to predict the scattered neutron momentum track hitting the PCAL/EC. We then search for PCAL/EC hits near the predicted position. We compare this predicted momentum track with the observed hit path, and if the angle between them, θ_{pq}, is within 1.5^o, this e-n event is considered found and we store it for later analysis.

6 Results

6.1 θ_{pq} Analysis

The angle θ_{pq} is the angle between the predicted 3-momentum vector and the measured 3-momentum vector. Figure 11 shows the resulting histograms from *e-n* θ_{pq} distributions. Figure 11a shows the expected angle results between the predicted 3-momentum vector using electron information and the found 3-momentum vector from generated events. Figure 11b shows the output after the simulation and reconstruction. Both distributions reach a peak near zero for QE events. The reconstructed data has a broader peak, and a cut on θ_{pq} can separate QE events from inelastic ones. This point will be necessary in helping us select QE events further in the analysis; we will choose *e-n* events that have a θ_{pq} less than 1.5^o.

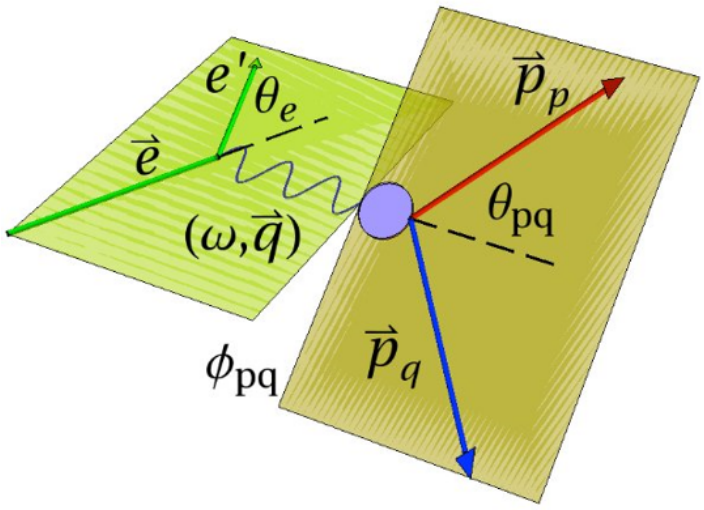

Figure 10: Using electron momentum plane information to extract θ_{pq}

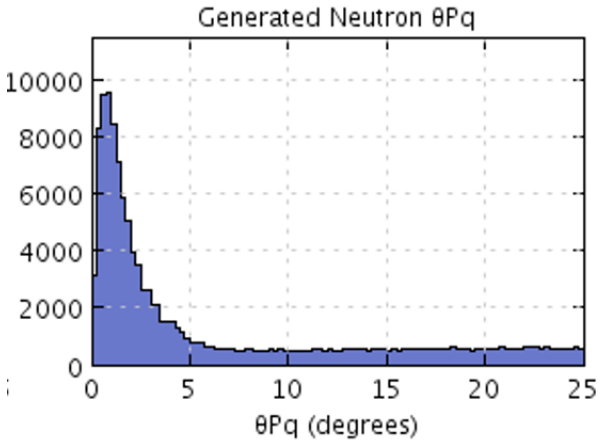

(a) Generated θ_{pq} histogram for e-n events

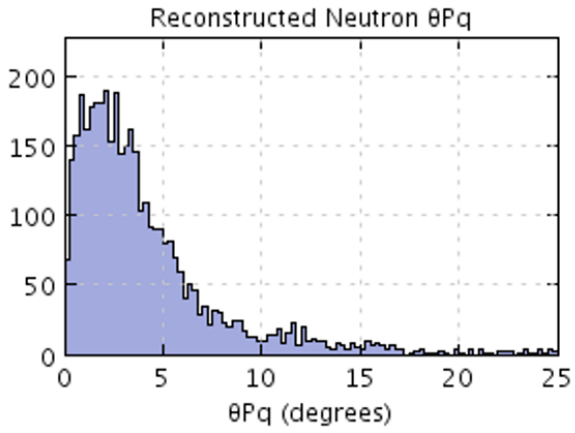

(b) Reconstructed θ_{pq} histogram for e-n events

Figure 11: θ_{pq} Generated vs Reconstructed

6.2 Elastic Scattering Angle vs Momentum Calibration

One check that we can do within our analysis is to make sure that our electron scattering angle versus momentum matches not only agrees with our generated simulation plots, but also theory. Plots of electron scattering angle versus momentum are shown in Figure 12a and 12b. Qualitatively, electrons appear to decrease in momentum with increased scattering angle, much like in Rutherford Scattering.

We also know through conservation of momentum laws that the electron scattering angle momentum is related to the scattering angle by the equation:

$$E' = \frac{E}{1 + 2\frac{E}{M_n}\sin^2\frac{\theta}{2}} \tag{1}$$

If we plot this theory curve on our reconstructed data plot, we can see that the data are consistent

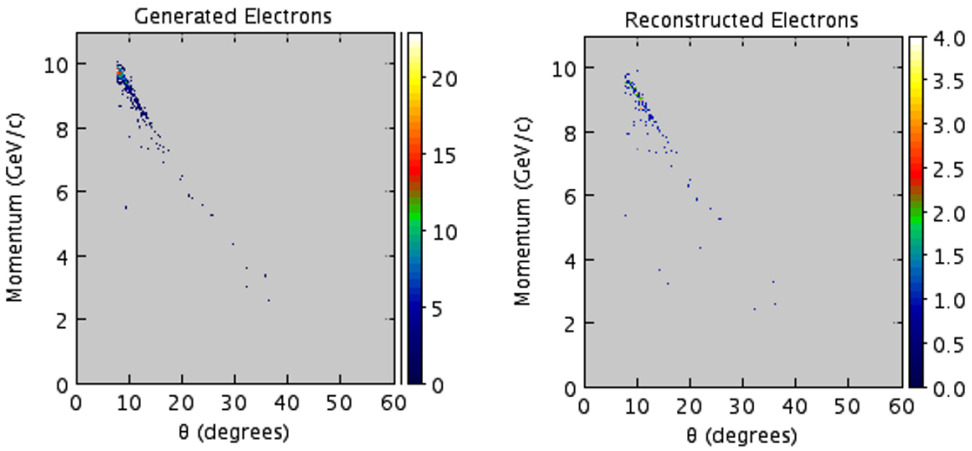

(a) Generated electron momentum vs scattering angle

(b) Reconstructed electron momentum vs scattering angle

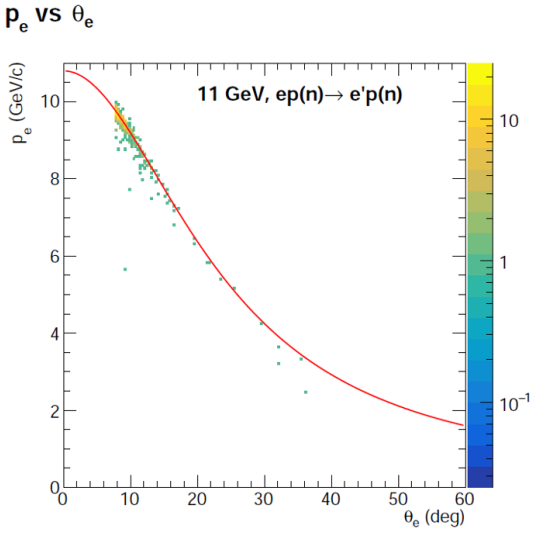

(c) Electron momentum vs scattering angle theory (red line) compared to our reconstructed data

Figure 12: Electron Momentum vs Scattering Angle

with QE scattering (Figure 12c). We observe a broad average above and below the red theory line. This is caused by the intrinsic fermi-motion of the deuterium target, which seemingly has slightly more or less energy than the initial 11 GeV beam.

6.3 Ratio

We are looking for a ratio, R, between the 4-momenta transfer of e-n events to e-p events. We have written an analysis code to extract R from the simulation and are now testing. Should the simulation prove successful, R can be used to extract the magnetic form factor of the neutron, G_m^n. The analysis is ongoing and not all corrections to R are currently in place.

6.3.1 Q^2 Distributions for e-n and e-p Events

Figure 13 shows the Q^2 distribution for e-n (left), peaking at about 6 GeV^2, and e-p (right), peaking at about 4.5 GeV^2. Both increase sharply at low Q^2 until they reach their peak.

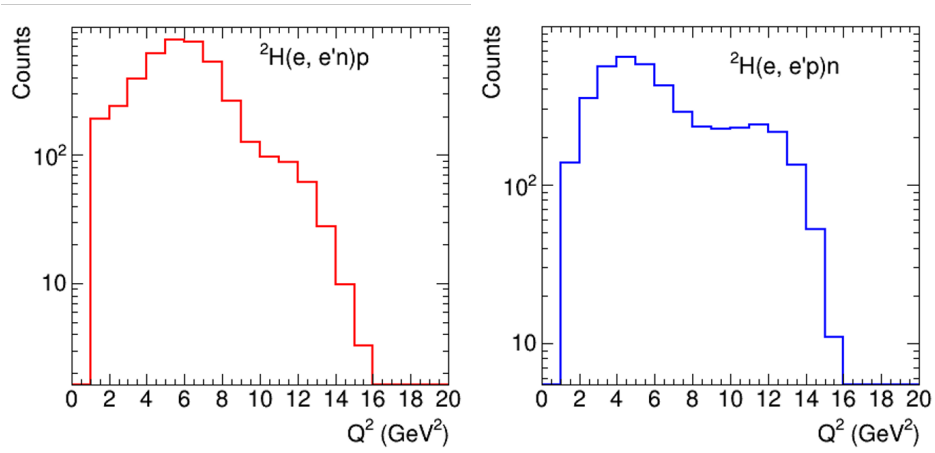

Figure 13: Q^2 distribution of *e-n* (left) and *e-p* (right)

6.3.2 e-n/e-p Q^2

Uncorrected R shown in Figure 14 is derived from the Figure 13 histograms. The average is roughly 0.7 which is larger than the expected 0.5-0.6 based on our simulation and previous measurements [5]. The variations are currently unexplained, and will be the subject of further investigation.

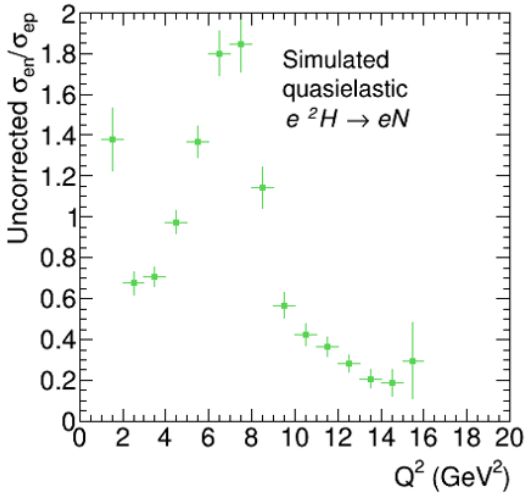

Figure 14: Uncorrected R

6.3.3 Using R to Calculate G_m^n

A relationship between $R_{corrected}$ and G_m^n is found to be

$$R_{corrected} = \frac{\sigma^n_{Mott}\left(G^2_{E,n} + \frac{\tau_n}{\epsilon_n}G^2_{M,n}\right)\left(\frac{1}{1+\tau_n}\right)}{\sigma^p_{Mott}\left(G^2_{E,p} + \frac{\tau_p}{\epsilon_p}G^2_{M,p}\right)\left(\frac{1}{1+\tau_p}\right)} \tag{2}$$

where,

$$\sigma_{Mott} = \frac{\alpha^2 E' \cos^2\left(\frac{\theta}{2}\right)}{4E^3 \sin^4\left(\frac{\theta}{2}\right)}$$

$$\tau = \frac{Q^2}{4M^2}$$

$$\epsilon = \left(1 + 2\left(1+\tau\right)\tan^2\left(\frac{\theta}{2}\right)\right)^{-1}$$

These quantities are all measurable, and known. The electric form factor of the neutron, G^n_E, is very small and almost negligible. If we reorient the expression, we can find the G^n_m in terms of one unknown, $R_{corrected}$.

$$G^n_M = \sqrt{\left[R_{corrected}\left(\frac{\sigma^p_{Mott}}{\sigma^n_{Mott}}\right)\left(\frac{1+\tau_n}{1+\tau_p}\right)\left(G^2_{E,p} + \frac{\tau_p}{\epsilon_p}G^2_{M,p}\right) - G^2_{E,n}\right]\frac{\epsilon_n}{\tau_n}} \tag{3}$$

7 Conclusion

We have successfully developed an end-to-end analysis from simulation to extraction of R in QE kinematics. The θ_{pq} analysis shows that a large number of e-n events have an angle within 1.5^o, allowing for better event selection. Reconstructed electron momentum versus scattering angle adheres to conservation of momentum laws and theory, supporting our simulation and analysis. Our final R is incorrect compared to previous measurements, and is the subject of further research. We are working to apply corrections to R by accounting for Neutron and Proton Detection Efficiencies (NDE and PDE), radiative corrections, and corrections for fermi-motion. We also need to further study the impact of background events that contaminate the QE peak.

8 Sources

References

[1] CLAS12. *Jefferson Lab Experimental Hall B.* N.p., n.d. Web. 27 Sept. 2016. <https://www.jlab.org/Hall-B/clas12-web/>.

[2] G.P.Gilfoyle et al *Measurement of the Neutron Magnetic Form Factor at High Q2 Using the Ratio Method on Deuterium.* E12-07-104 Jefferson Lab, Newport News, VA, 2007.

[3] G.P. Gilfoyle and O. Alam. *QUEEG: A Monte Carlo Event Generator for Quasi-Elastic Scattering on Deuterium.* CLAS12-NOTE 2017-007, Jefferson Lab, 2014

[4] Gilfoyle, G. P., and M. Ungaro. *Simulating the Electromagnetic Calorimeter in CLAS12.* (n.d.):n. pag. Web. <¡https://facultystaff. richmond.edu/ ggilfoyl/research/clas12Mar10ECtalk.pdf¿.>

[5] J. Lachniet et al. *"Precise Measurement of the Neutron Magnetic Form Factor G_m^n in the Few-GeV^2 Region.* Phys. Rev. Lett, 102, 192001, 2009.

[6] Stepanvan, S. *CLAS12-Preshower Calorimeter (PCAL).* (n.d.):n. pag. Web. <https://www.jlab.org/Hall-B/clas12-web/specs/pcal.pdf>.